

Operational performance of the CMS silicon strip detector during Run 3

Ivan Shvetsov^{a,*} on behalf of the CMS collaboration

^a*Karlsruhe Institute of Technology*

E-mail: ivan.shvetsov@cern.ch

The CMS silicon strip tracker, consisting of 15148 silicon modules with a 198 m² active area, has been successfully taking data in LHC Run 1 and Run 2. After the second long shut-down period from the end of 2018, the detector resumed operations in summer 2021 and will be operational till the end of LHC Run 3, before the HL-LHC upgrade. The performance of the detector during Run 3 will be discussed, with particular emphasis on the (expected) changes in detector performance with increasing irradiation. The performance of the detector during the early 2023 collisions will also be presented.

*The 32nd International Workshop on Vertex Detectors (VERTEX2023)
16-20 October 2023
Sestri Levante, Genova, Italy*

*Speaker

1. Introduction

The Silicon Strip Tracker (SST) is positioned at the heart of the CMS experiment at the LHC [1]. Together with the pixel detector it measures charged particle trajectories up to a pseudorapidity of $|\eta| < 2.5$. Fig. 1 illustrates the configuration of the SST.

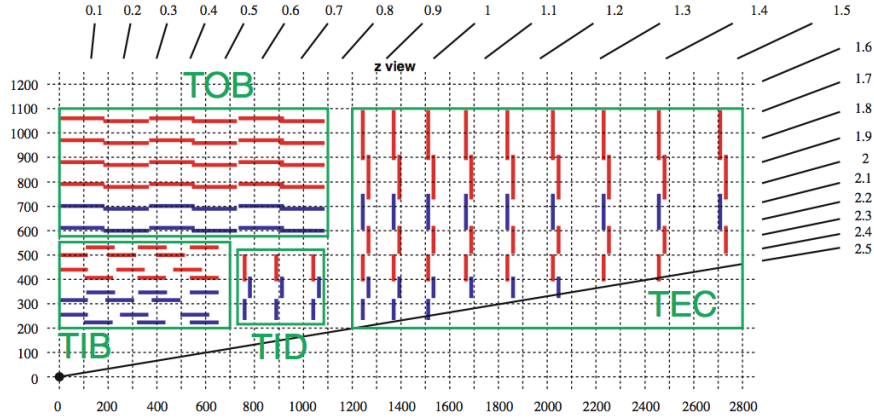


Figure 1: The layout of the CMS Silicon Strip tracker [2].

The SST, 5 meters in length and 2.5 meters in diameter, comprises 9.3 million strips and covers an active silicon area of 198 m^2 , spread across 15 148 modules. Single-sided p-on-n micro-strip sensors are utilized. The modules are assembled in either layers or rings. The SST includes ten layers situated in the barrel region, housing four layers within the Tracker Inner Barrel (TIB) and six layers within the Tracker Outer Barrel (TOB). Additionally, the TIB incorporates 3 Tracker Inner Disks (TID) at either end. In the forward region, the detector comprises Tracker End-Caps (TEC) at both ends, illustrated in Fig. 1. Each TID consists of 3 rings, while the disks in each TEC have 4–7 rings.

In the TIB, TID, and the first 4 rings of the TEC, sensors with thickness of $320 \mu\text{m}$ are utilized, while in the TOB and in rings 5–7 of the TEC there are $500 \mu\text{m}$ sensors (Fig. 2). Within the four layers of the barrel and across two rings of the inner disks and three rings of the end-caps, special stereo modules are used (indicated by blue lines in Fig. 1). These particular modules consist of a second module affixed in a back-to-back configuration, featuring a stereo angle of 100 mrad . Their purpose is to ascertain measurements of 3D coordinates, specifically the radial coordinate (r) in the disks and the longitudinal coordinate (z) in the barrel.

The signals originating from sensors undergo processing via APV25 chips [3], subsequently transitioning into optical signals through analog-opto-hybrids (AOH). These optical signals are then conveyed to front-end drivers (FEDs) situated in the service cavern outside the radiation zone via optical fibers. Within the FEDs processes such as pedestal and common mode subtraction along with cluster identification take place.

For synchronization purposes clock and trigger information is propagated by front-end controllers (FEC) to Communication and Control Units (CCU) assembled in token ring networks, also known as control rings.

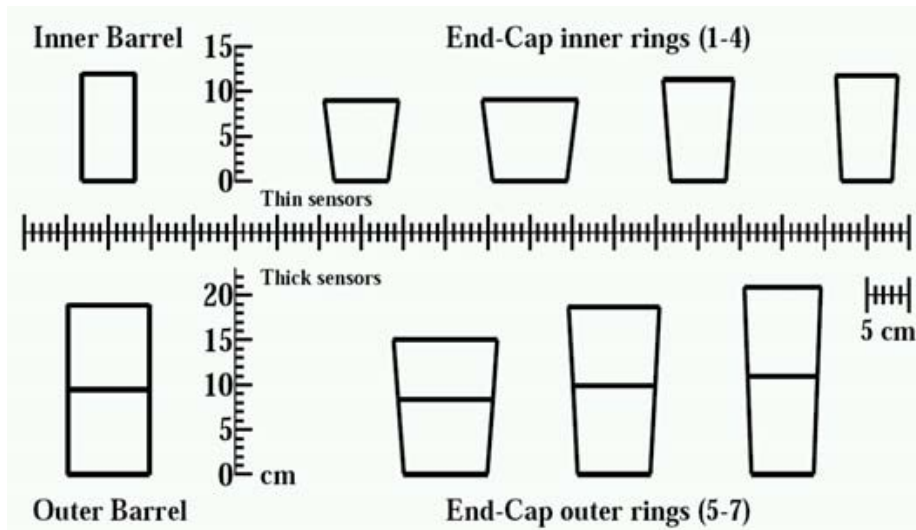


Figure 2: Geometry of sensors used in the CMS Strip Tracker [1].

Regarding its power infrastructure, the SST consists of 1944 power groups. Each power group comprises 2 low voltage channels equipped with 2.5 V and 1.25 V regulators respectively, alongside 2 high voltage channels that can be adjusted to levels up to 600 V [1]. The detector is cooled using a monophasic coolant, specifically C_6F_{14} , managed by two cooling plants.

2. Run 3 experience

2.1 Detector status

The fraction of active readout channels in the detector is about 96% and has been largely stable since the spring of 2015. The tracker map shown in Fig. 3 illustrates the distribution of inactive channels in the detector. Components excluded from data-taking include failing control rings,

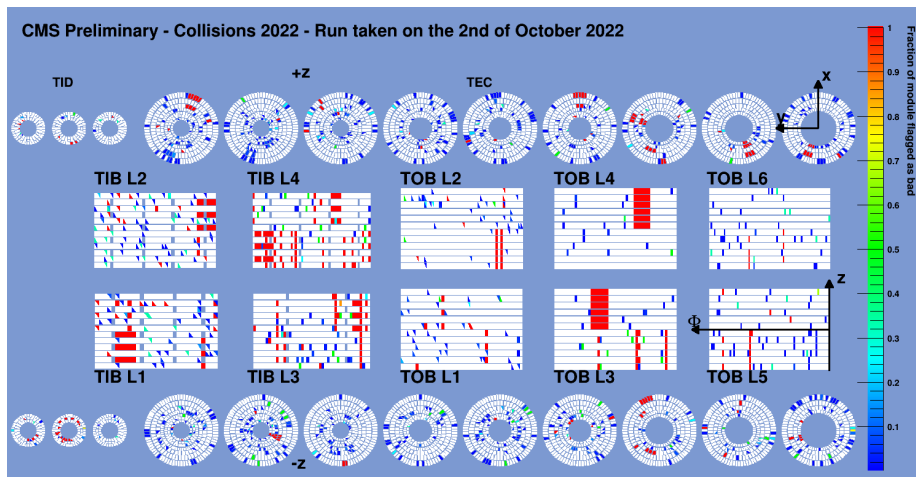


Figure 3: Tracker map illustrating inactive channels in the detector [4].

problems in LV or HV distribution, and individually switched-off modules.

In the beginning of 2022, two cooling loops (in one cooling station) were closed because of a leak. The exact reason for the leak remains unknown. Also, in June 2023 the operational temperature has been lowered from -20°C to -22°C . Figure 4 demonstrates the silicon temperature in the SST in July 2023, when the coolant temperature was set at -22°C . Hot spots in the TIB layer 1 and layer 2 correspond to the regions with degraded cooling contacts. Also hot regions in TIB layer 3 and TOB layer 3 as well as TID– disk 2 correspond to closed loops. Hot regions in TEC+ disk 1, 3, 5, 7 and TIB layer 4 correspond to loops that were closed in 2022. Purple regions correspond to modules where no data has been sent by Detector Control Unit (DCU). Gray regions correspond to modules excluded from the data-taking.

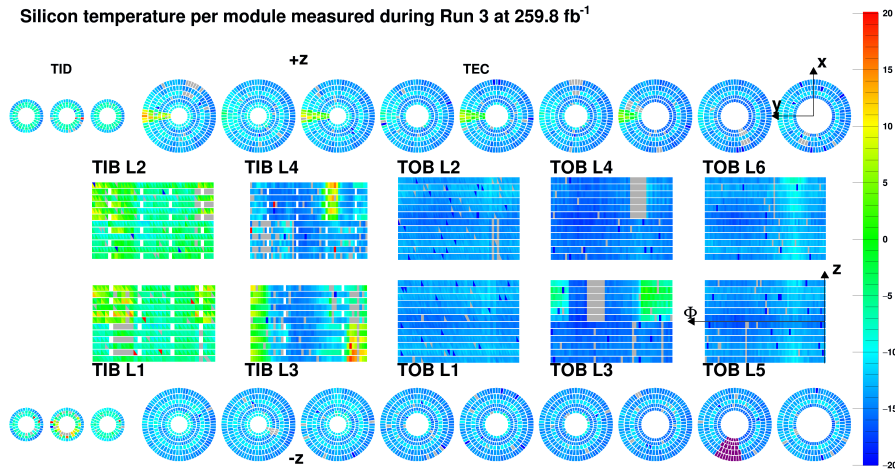


Figure 4: Tracker map illustrating silicon temperatures channels in the detector [5].

2.2 Detector performance

The performance of the Strip Tracker is monitored continuously. One of the most important characteristics of the detector is the signal-to-noise ratio (S/N) of hits. The signal-to-noise distributions for the TIB and TOB are shown in Fig. 5. Each distribution can be fitted with a Landau convoluted with a normal distribution.

The evolution of the S/N with integrated luminosity is shown in Fig. 6. As expected from irradiation studies [6], the S/N drops with integrated fluence. Furthermore, the curve follows the expected trend. Based on the data collected so far, we estimate that S/N of the Strip Tracker will be sufficient for high quality physics data taking up to the end of its operational lifetime ($\sim 500 \text{ fb}^{-1}$).

The single hit efficiency is measured as a function of the instantaneous luminosity. Tracks passing so-called high purity criteria [8] of the tracking algorithm are used for the measurement. If the trajectory starts or ends with a considered module, it is discarded for computing the efficiency of that module. Thus, measurement in the first layer, TIB layer 1, relies on pixel seeding and moreover no measurement is possible in the outermost regions, i.e., TOB layer 6 and TEC disk 9. Hit efficiency is measured with a standard bunch fill with luminosity below $1.8 \cdot 10^{34} \text{ Hz/cm}^2$ and high luminosity fills with luminosity over $1.8 \cdot 10^{34} \text{ Hz/cm}^2$. It can be seen in Fig. 7 that the hit efficiency scales linearly with the instantaneous luminosity (pileup). It is greater than 98% and depends on the

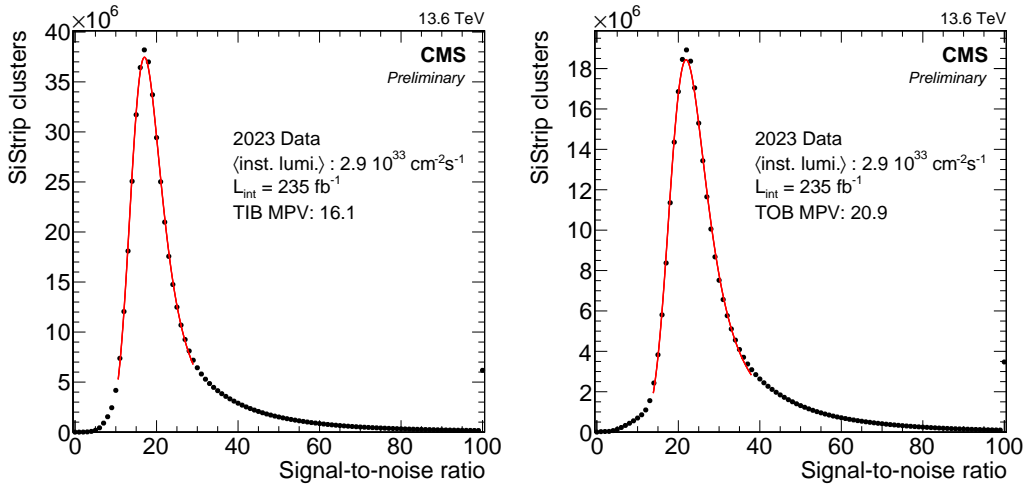


Figure 5: Signal-to-noise distribution for hits on reconstructed particle tracks for TIB (left) and TOB (right).

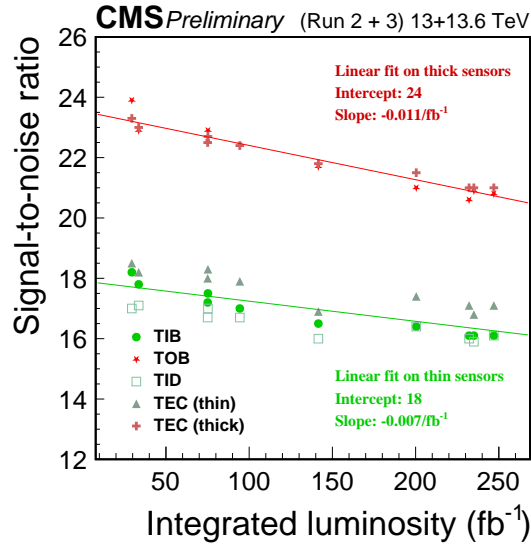


Figure 6: S/N as a function of integrated luminosity [7].

layer of the detector. Layers are affected differently because of the different probability of Highly Ionizing Particles (HIP)¹ to pass the silicon sensors [9].

An estimation of the hit resolution is performed with the so-called pair method based on tracks passing the detector through overlapping modules from the same tracking layer. Tracks with $p_T > 3$ GeV/c, at least 6 hits in the strip tracker and χ^2 track fit probability $> 10^{-3}$ are selected. Clusters of the same size are considered. The resolution is computed as:

$$\sigma_{\text{hit}} = \frac{\sqrt{\sigma_{\text{meas-pred}}^2 - \sigma_{\text{pred}}^2}}{\sqrt{2}} \quad (1)$$

¹HIPs are particles that can deposit the energy equivalent of ~ 100 Minimum Ionizing Particles (MIP).

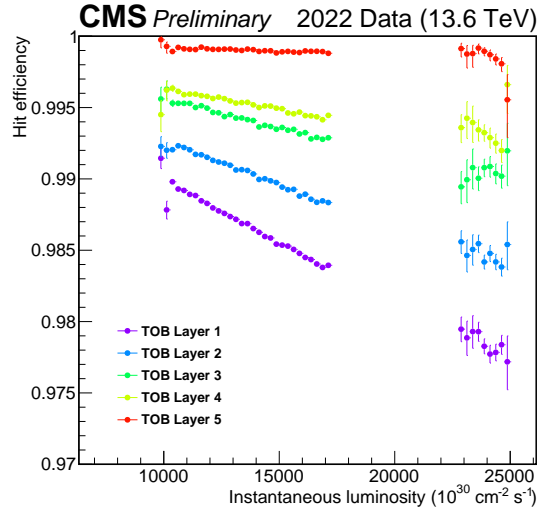


Figure 7: Single hit efficiency of silicon strip modules from five TOB layers as a function of the instantaneous luminosity [10].

where σ_{pred} is extracted from the fit of difference in predicted hit positions to normal distribution, and $\sigma_{\text{meas-pred}}$ is extracted from the fit of double difference of measured and predicted hit positions to the normal distribution [8]. The measured hit resolution is shown in Fig. 8, where resolution of a hypothetical binary readout is shown for comparison, demonstrating that the hit resolution of the SST benefits from charge sharing in conjunction with the analog readout .

3. Radiation effects

By the end of proton-proton collisions in 2023 the CMS Strip Tracker had received a radiation dose corresponding to integrated luminosity of 266 fb^{-1} . Radiation effects are continuously monitored and they include: increase in leakage current, change of full depletion voltage due to the change of effective sensor doping concentration, and evolution of laser driver performance in the optical readout chain.

Leakage current is measured both with the DCUs and power supply units [1]. In 2023 some of the modules in uncooled regions reached quite high leakage current, with a few modules in TIB layer 1 exceeding 2 mA (the power limit is 12 mA for 6 modules). Only few thermal runaways, similar to the one mentioned in [9], were observed in 2023. In order to decrease the leakage current in the modules with high leakage current, the operational temperature has been lowered to -22°C .

It can be seen from Fig. 9 that only modules regions with degraded cooling contact or closed loops have high leakage currents and other modules are well below the power supply limit.

The full depletion voltage is measured during bias scans of the full detector (taken twice per year) and bias scans of selected modules (taken once per month). The expected full depletion voltages of the strip detector modules are calculated using the Hamburg model [11]. In Fig. 10 the evolution of the full depletion voltage for TIB layer 1 is shown. Predictions are given for a hypothetical module with characteristics (initial full depletion voltage and temperature) representative of

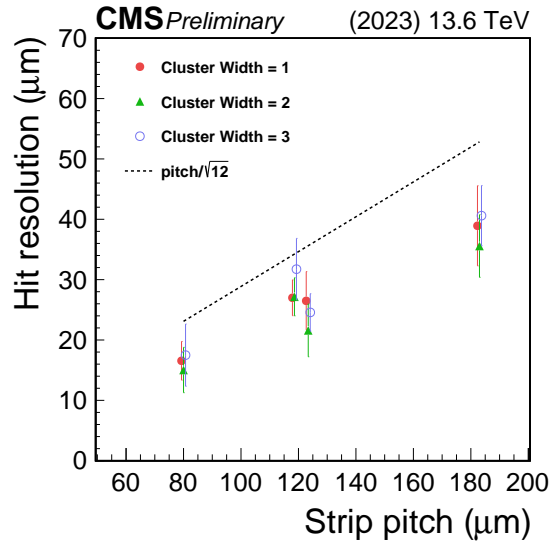


Figure 8: Strip hit resolution derived with the pair method by selecting pairs of hits in different types of overlapping sensors and for different cluster widths expressed in units of number of strips. The expected resolution for a hypothetical binary readout ($\text{pitch}/\sqrt{12}$) is also shown for comparison, demonstrating the benefit from charge sharing due to the analog readout [7].

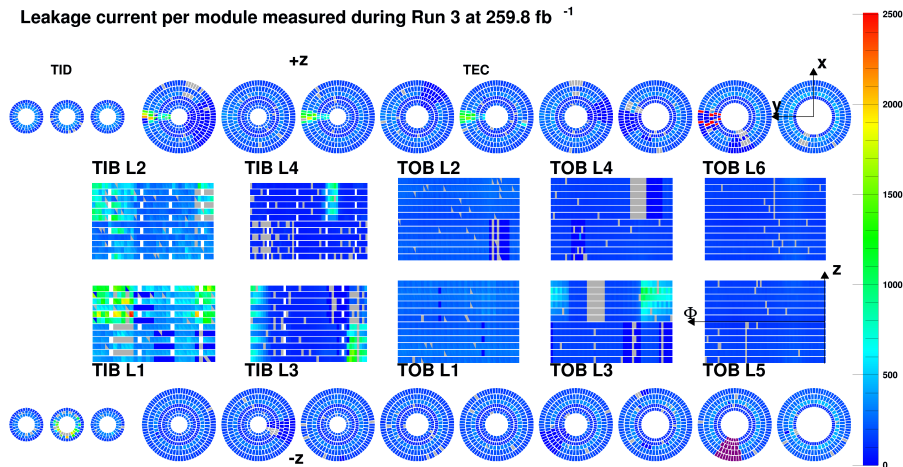


Figure 9: Tracker map illustrating leakage current in the SST[5]. Purple regions correspond to problems with the slow local control readout. Gray regions correspond to modules excluded from the data-taking.

all the modules of the layer. The values for the full depletion voltage before April 2023 (red-dashed line) are computed using the measured integrated luminosity and the actual temperature of the detector. Then, the full depletion voltage is computed using the expected integrated luminosity and temperature after April 2023, in particular for Run 3, a scenario with 260 fb^{-1} is used. The effective doping type inversion from n to p is observed at the end of Run 2 for TIB L1. Currently modules in TIB layer 1 have a full depletion voltage of about 100 V.

In Fig. 11 initial and final (predicted) values of the full depletion voltage are presented. The initial values (red squares) are determined by the capacitance versus voltage scan at the time of

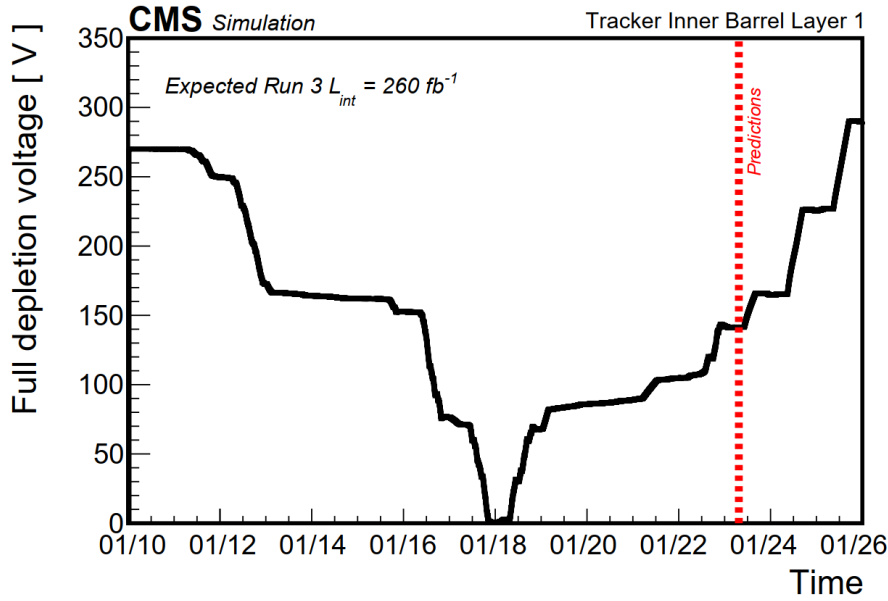


Figure 10: The CMS Strip Tracker full depletion voltage plot for TIB layer 1 as a function of time [12]. The evolution of full depletion voltage after April 2023 (indicated with red dashed line) is computed using the expected integrated luminosity and temperature.

the module construction. Predictions are given for an hypothetical module with characteristics representative of all the modules of the layer. The final values (blue dots) are the values expected at the end of Run 3 from the Hamburg Model. With the limit of 600 V limit in the power system there is enough margin to operate the modules fully depleted until the end of Run 3.

Radiation effects in the optical readout include the increase of the laser driver threshold (minimum current needed to get non-zero signal from the laser diode) and a loss of efficiency of a laser. The evolution of the laser driver current threshold increase is shown in Fig. 12 for different layers of the TIB. As can be seen in Fig. 12, the current laser driver threshold increases with irradiation during data-taking and anneals during end-of-year technical stops. The threshold current also decreases when the operational temperature is changed from -15°C to -20°C during Run 2 and and from -20°C to -22°C during Run 3. The average current at the time of reference was about 3 mA and the maximum allowed current is 22.5 mA, which indicates that the optical system of the tracker will have quite some margin for operation even at the end of Run 3.

4. Summary and outlook

The CMS Silicon Strip Tracker is performing well during Run 3 after more than ten years of operation. Together with the other subsystems of the CMS experiment it continues to deliver high quality data for physics analyses. The system has not shown any significant degradation over the last years. The signal-to-noise ratio, hit efficiency, and hit resolution are very good and compatible with the expectations. The operational temperature of the detector has been changed from -20°C to -22°C , which helped to decrease the leakage current in regions with degraded cooling. The detector

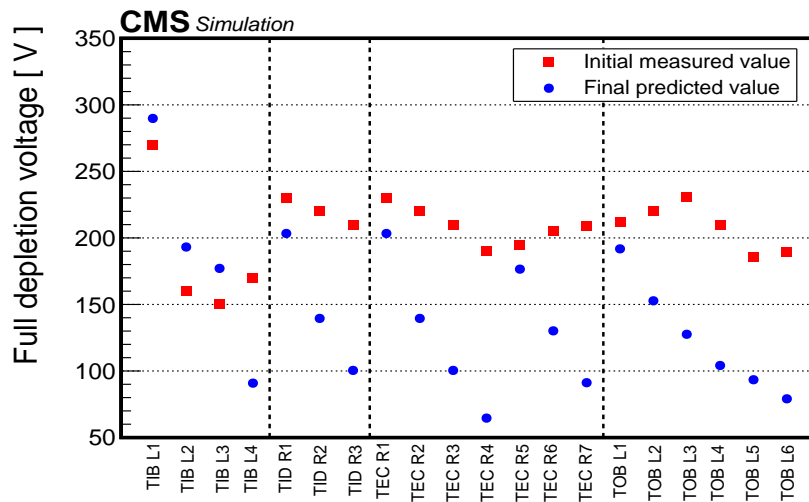


Figure 11: The CMS Strip Tracker full depletion voltage summary plot for the different layers : TIB, TID, TEC, and TOB[12].

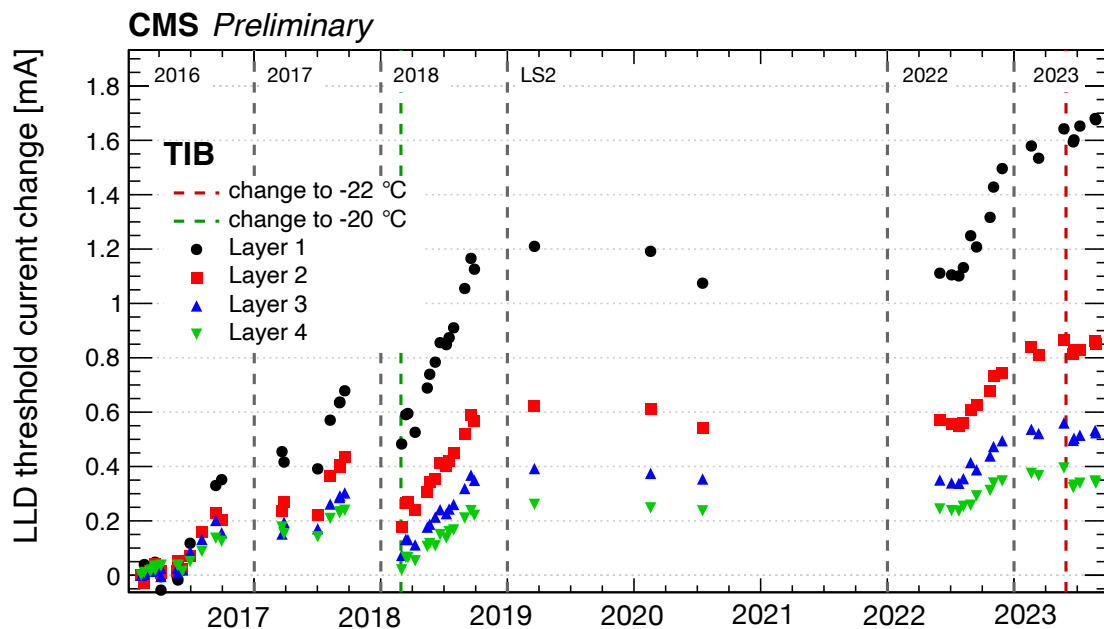


Figure 12: Evolution of the laser driver current threshold in the TIB as a function of time [13].

was recalibrated and commissioned at the new operational temperature in June 2023. Radiation effects are monitored continuously and are visible in all parts of the detector. The first layer of the TIB has passed the space charge inversion point and now has a full depletion voltage of about 100 V. In order to lower the leakage currents in the regions with degraded cooling contacts the operational temperature will be eventually lowered to -25°C , but given the strong dependence of the cooling system leak with temperature this will be postponed as long as possible.

References

- [1] CMS Collaboration, "*The CMS experiment at the CERN LHC*" JINST 3 (2008) S08004.
- [2] F. Hartman, *Evolution of Silicon Sensor Technology in Particle Physics*, Springer International Publishing AG, 2017, DOI 10.1007/978-3-540-44774-0.
- [3] M. J. French *et al.*, "*Design and results from the APV25, a deep sub-micron CMOS front-end chip for the CMS tracker*" Nucl. Instrum. Meth. A 466, p.359 (2001).
- [4] CMS Collaboration, "*Bad components of the CMS Silicon Strip Tracker with early Run 3 data*", CMS-DP-2022-048, <https://cds.cern.ch/record/2839742>, 2022.
- [5] CMS Collaboration, "*CMS Silicon Strip Tracker Maps*", CMS-DP-2023-083, <https://cds.cern.ch/record/2879281>, 2023.
- [6] W. de Boer *et al.*, "*The performance of irradiated CMS silicon micro-strip detector modules*", CMS-NOTE-2006-049, <http://cdsweb.cern.ch/record/951391>.
- [7] CMS Collaboration, "*CMS Silicon Strip Tracker Performance in 2023*", CMS-DP-2023-040, <http://cds.cern.ch/record/2865841>, 2023.
- [8] CMS Collaboration, "*Description and performance of track and primary-vertex reconstruction with the CMS tracker*" JINST 9 (2014), P10009.
- [9] I. Shvetsov [CMS], "Operational experience with the Silicon Strip Tracker at the CMS experiment," PoS VERTEX2018 (2019), 003 doi:10.22323/1.348.0003.
- [10] CMS Collaboration, "*CMS Silicon Strip Tracker Performance Results in 2022*", CMS-DP-2023-030, <https://cds.cern.ch/record/2860872>, 2023.
- [11] M. Moll, Radiation "*Damage in Silicon Particle Detectors*", Universität Hamburg, DESY-THESIS-1999-040, 1999, <https://mmoll.web.cern.ch/mmoll/thesis/>.
- [12] CMS Collaboration, "*Full Depletion Voltage Prediction for CMS Silicon Strip Tracker in Run 3*", CMS-DP-2023-082, <https://cds.cern.ch/record/2879280>, 2023.
- [13] CMS Collaboration, "*CMS Silicon Strip Tracker Linear Laser Driver Thresholds versus time*", CMS-DP-2023-084, <https://cds.cern.ch/record/2879282>, 2023.